

In conclusion, by determining the solution structure of **1**, we have demonstrated that *N,N'*-linked oligoureas of general formula **B** belong to the growing family of non-natural non-peptide oligomers with defined and predictable secondary structures. Although heptaurea **1** forms a (*P*)2.5 helix of approximately 5.1 Å pitch that is closely related to the (*P*)2.6<sub>14</sub> helix of approximately 5 Å pitch of corresponding  $\gamma^4$ -peptides,<sup>[4a]</sup> it is worth noting that both NH groups within the same urea linkage may participate in intramolecular hydrogen bonding to the same C=O group. The knowledge of the three-dimensional structure of **1** is likely to be useful for the de novo design of oligoureas with controlled shape and defined biological activities.

Received: October 1, 2001 [Z17991]

- [1] S. H. Gellman *Acc. Chem. Res.* **1998**, *31*, 173–180; K. Kirshenbaum, R. N. Zuckermann, K. A. Dill, *Curr. Opin. Struct. Biol.* **1999**, *9*, 530–535.
- [2] For representative examples of helical  $\beta$ -peptides, see D. Seebach, M. Overhand, F. N. M. Kühnle, B. Martinoni, L. Oberer, U. Hommel, H. Widmer, *Helv. Chim. Acta* **1996**, *79*, 913–941; D. Seebach, S. Abele, K. Gademann, G. Guichard, T. Hintermann, B. Jaun, J. L. Matthews, J. V. Schreiber, L. Oberer, U. Hommel, H. Widmer, *Helv. Chim. Acta* **1998**, *81*, 932–982; S. Abele, G. Guichard, D. Seebach, *Helv. Chim. Acta* **1998**, *81*, 2141–2156; D. Seebach, T. Sifferlen, P. A. Mathieu, A. M. Häne, C. M. Krell, D. J. Bierbaum, S. Abele, *Helv. Chim. Acta* **2000**, *83*, 2849–2864; H. Appella, L. A. Christianson, I. L. Karle, D. R. Powell, S. H. Gellman, *J. Am. Chem. Soc.* **1996**, *118*, 13071–13072; D. H. Appella, L. A. Christianson, D. A. Klein, D. R. Powell, X. Huang, J. J. Barchi, Jr., S. H. Gellman, *Nature* **1997**, *387*, 381–384; D. H. Appella, J. J. Barchi, Jr., S. R. Durell, S. H. Gellman, *J. Am. Chem. Soc.* **1999**, *121*, 2309–2310; X. Wang, J. F. Espinosa, S. H. Gellman, *J. Am. Chem. Soc.* **2000**, *122*, 4821–4822.
- [3] For representative examples of sheet and turn structures with  $\beta$ -peptides, see a) D. Seebach, S. Abele, K. Gademann, B. Jaun, *Angew. Chem.* **1999**, *111*, 1700–1703; *Angew. Chem. Int. Ed.* **1999**, *38*, 1595–1597; b) S. Krauthäuser, L. A. Christianson, D. R. Powell, S. H. Gellman, *J. Am. Chem. Soc.* **1997**, *119*, 11719–11720; c) Y. J. Chung, R. B. R. Huck, L. A. Christianson, H. E. Stanger, S. Krauthäuser, D. R. Powell, S. H. Gellman, *J. Am. Chem. Soc.* **2000**, *122*, 3995–4004.
- [4] For leading references on  $\gamma$ -peptides, see a) T. Hintermann, K. Gademann, B. Jaun, D. Seebach, *Helv. Chim. Acta* **1998**, *81*, 983–1002; b) D. Seebach, M. Brenner, M. Rueping, B. Schweizer, B. Jaun, *Chem. Commun.* **2001**, 207–208; c) S. Hanessian, X. Luo, R. Schaum, S. Michnick, *J. Am. Chem. Soc.* **1998**, *120*, 8569–8570; d) S. Hanessian, X. Luo, R. Schaum, *Tetrahedron Lett.* **1999**, *40*, 4925–4929.
- [5] a) K. Burgess, D. S. Linthicum, H. Shin, *Angew. Chem.* **1995**, *107*, 975–977; *Angew. Chem. Int. Ed. Engl.* **1995**, *34*, 907–908; b) K. Burgess, J. Ibarzo, D. S. Linthicum, D. H. Russell, H. Shin, A. Shitangkoon, R. Totani, A. J. Zhang, *J. Am. Chem. Soc.* **1997**, *119*, 1556–1564.
- [6] a) J. M. Kim, Y. Bi, S. Paikoff, P. G. Schultz, *Tetrahedron Lett.* **1996**, *37*, 5305–5308; b) A. Boeijen, R. M. J. Liskamp, *Eur. J. Org. Chem.* **1999**, 2127–2135; c) G. Guichard, V. Semetey, C. Didierjean, A. Aubry, J. P. Briand, M. Rodriguez, *J. Org. Chem.* **1999**, *64*, 8702–8705; d) G. Guichard, V. Semetey, M. Rodriguez, J. P. Briand, *Tetrahedron Lett.* **2000**, *41*, 1553–1557.
- [7] Similarly, Seebach and co-workers have shown in the case of a  $\beta$ -heptapeptide that  $J(\text{NH},\beta\text{CH})$  values decrease only slowly upon an increase of the temperature from 298 to 353 K. A decrease of about 0.4 Hz was observed for the central residues (3–6) and about 0.7 Hz for the flanking residues 2 and 7: K. Gademann, B. Jaun, D. Seebach, R. Perozzo, L. Scapozza, G. Folkers, *Helv. Chim. Acta* **1999**, *82*, 1–11.
- [8] In the case of residue 3,  $^3J(\alpha\text{CH}_2,\text{NH})$  values were extracted directly from the 1D NMR spectrum, but decoupling experiments were required to access precise  $^3J(\beta\text{CH},\alpha\text{CH}_2)$  values. Severe overlaps in the  $\alpha\text{CH}$  region precluded measurement of the  $^3J(\beta\text{CH},\alpha\text{CH}_2)$  values for other residues. However, qualitative examination of the COSY spectrum reveals similar vicinal coupling patterns.
- [9] D. A. Case, D. A. Pearlman, J. W. Caldwell, D. E. Cheatham III, W. S. Ross, C. L. Simmerling, T. A. Darden, K. M. Merz, R. V. Stanton, A. L. Cheng, J. J. Vincent, M. Crowley, V. Tsui, R. J. Radmer, Y. Duan, J. Pitera, I. Massova, G. L. Seibel, U. C. Singh, P. K. Weiner, P. A. Kollman, AMBER6, University of California, San Francisco, **1999**
- [10] Further experimental evidence for  $\text{C}=\text{O}_i\cdots\text{HN}'_{i+2}$  and  $\text{C}=\text{O}_i\cdots\text{HN}_{i+3}$  hydrogen bonds is gained from the determination of temperature coefficients.  $\text{N}'\text{H}_{i+2}$  for  $i=1-4$  and  $\text{NH}_{i+3}$  for  $i=1-4$  have temperature coefficients with absolute values  $<4$  ppb  $\text{K}^{-1}$ , which indicates limited solvent accessibility. In addition, temperature coefficients of  $\text{N}'\text{H}_{i+2}$  for  $i=2-4$  ( $3.5$  ppb  $\text{K}^{-1} < -\Delta\delta/\Delta T < 3.8$  ppb  $\text{K}^{-1}$ ) have higher absolute values than those of  $\text{NH}_{i+3}$  for  $i=2-4$  ( $1.5$  ppb  $\text{K}^{-1} < -\Delta\delta/\Delta T < 2.5$  ppb  $\text{K}^{-1}$ ). This trend could suggest an increased solvent accessibility for  $\text{N}'\text{H}_{i+2}$  compared to  $\text{NH}_{i+3}$ .

## Self-Assembling Organic Nanotubes from Enantiopure Cyclo-*N,N'*-Linked Oligoureas: Design, Synthesis, and Crystal Structure

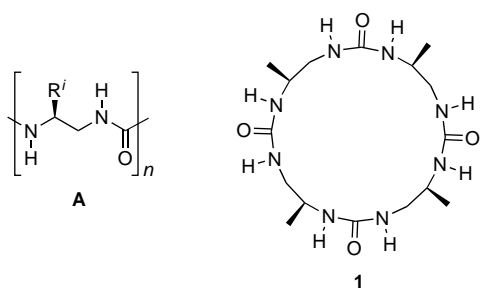
Vincent Semetey, Claude Didierjean, Jean-Paul Briand, André Aubry, and Gilles Guichard\*

Assembly of self-complementary cyclo-oligomeric subunits through noncovalent processes (for example, hydrogen bonding, aromatic stacking) has emerged as a powerful strategy to generate artificial organic nanotubular structures.<sup>[1,2]</sup> Highly functionalized tubular assemblies based on peptides have attracted much interest recently in this area. Ghadiri and co-workers have compellingly demonstrated that 24- and 30-membered-ring cyclo- $\alpha$ -peptides with an even number of alternating D- and L-amino acids stack in an antiparallel  $\beta$ -sheet-like arrangement to form hydrogen-bonded tubular structures, that is, “peptide nanotubes”.<sup>[2–4]</sup> Remarkably, related cyclic peptides consisting exclusively of  $\beta$ -amino acids<sup>[5,6]</sup> (16- and 12-membered ring), of alternating  $\alpha$ - and  $\beta$ -amino acids<sup>[7]</sup> (14-membered ring), or of vinylogous  $\delta$ -amino acids<sup>[8]</sup> (18-membered ring) also form tubular stacks.

We have shown previously<sup>[9]</sup> that linear *N,N'*-linked oligoureas **A** consisting of homochiral residues adopt a stable 2.5-helical secondary structure in solution. The helix is characterized by the simultaneous presence of 12- and 14-membered hydrogen-bonded rings resulting from the capacity of the urea group to establish self-complementary bidirec-

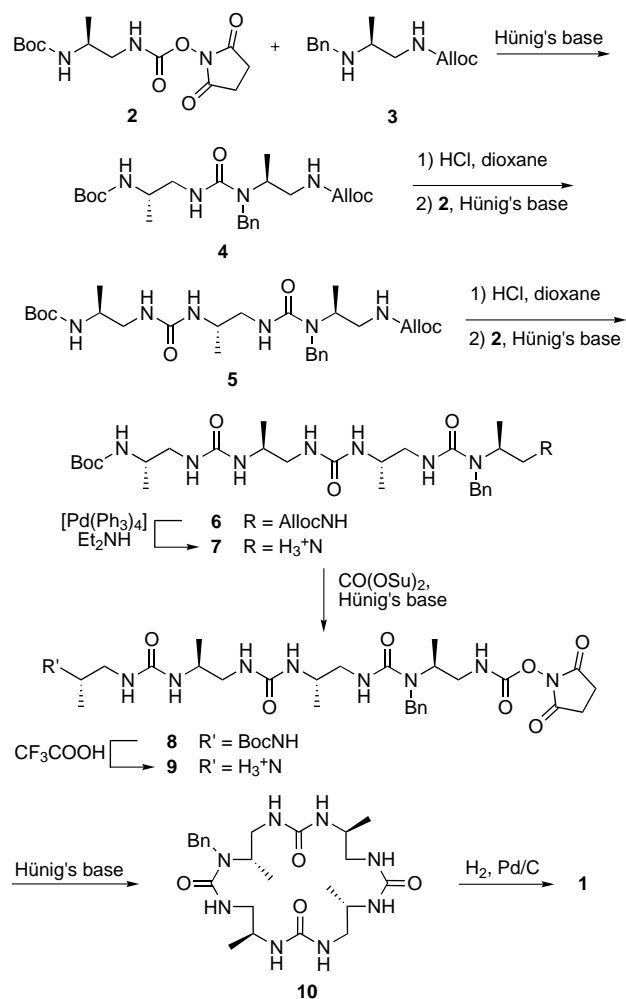
[\*] Dr. G. Guichard, V. Semetey, Dr. J.-P. Briand  
Immunologie et Chimie Thérapeutiques, UPR CNRS 9021  
Institut de Biologie Moléculaire et Cellulaire  
15, rue Descartes, 67084 Strasbourg (France)  
Fax: (+33) 3-88-61-06-80  
E-mail: G.Guichard@ibmc.u-strasbg.fr  
Dr. C. Didierjean, Dr. A. Aubry  
LCM3B, UMR-CNRS 7036, Groupe Biocristallographie  
Université Henri Poincaré  
BP 239, 54506 Vandœuvre, France

Supporting information for this article is available on the WWW under <http://www.angewandte.com> or from the author.



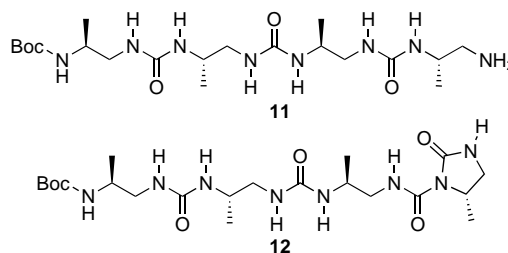
tional intermolecular hydrogen bonds. We envisioned that the corresponding macrocyclic derivatives might lead to flat ring structures with a high degree of self-complementarity that would allow self-assembling processes to occur. Herein we report the design and the synthesis of the  $C_4$ -symmetric (all-*S*) cyclotetraurea **1** bearing side chains of alanine, and demonstrate by single-crystal X-ray analysis that **1** forms square-shaped nanotubes.

The general stepwise strategy used to synthesize the 20-membered-ring macrocycle **1** is outlined in Scheme 1. Reac-



Scheme 1. Synthesis of **1**. Alloc = allyloxycarbonyl, Boc = *tert*-butoxycarbonyl, Bn = benzyl, Hünig's base = diisopropylethylamine, Su = succinimidyl.

tion of the succinimidyl carbamate derivative **2**<sup>[10]</sup> with the monoprotected benzylated diamine **3** yielded the trisubstituted urea **4**. Removal of the Boc group followed by urea formation with **2** gave the bisurea **5**. Repetition of this two-step sequence gave the fully protected triurea **6** in an overall yield of 45% from **3**. Following quantitative removal of the Alloc group, the resulting amine **7** was converted into the key activated linear precursor **8** by treatment with di(*N*-succinimidyl carbonate). At this stage, the temporary protection of the urea with a benzyl group was mandatory. Initial attempts to convert the linear oligotriurea precursor **11** under the same conditions were not successful and led exclusively to the formation of the cyclic biuret derivative **12**.



The Boc protecting group was selectively removed upon treatment of crude **8** with  $\text{CF}_3\text{COOH}$  to give the trifluoroacetate salt **9**. Slow addition of a solution of **9** in MeCN to a dilute solution of Hünig's base in MeCN resulted in the formation of the expected monobenzylated cyclic oligotetraurea **10** in a yield of 62% from **7** after HPLC purification ( $\text{C}_{18}$  column, reversed phase). Cyclotetraurea **1** was obtained in 92% yield from **10** following deprotection of the urea group by hydrogenation in EtOH. Single crystals of **1** suitable for X-ray studies were grown by slow evaporation of the EtOH solution.

X-ray crystallographic analysis<sup>[11]</sup> revealed that cycloureia **1** adopts a  $C_4$ -symmetric conformation in the solid state and stacks to form a hollow tubular structure (Figure 1). The four

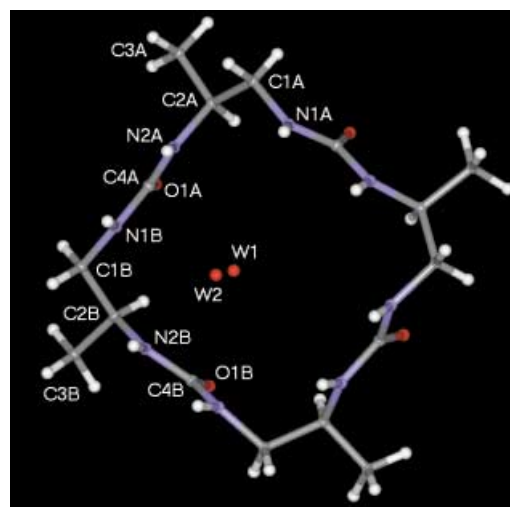


Figure 1. Ball and stick representation of **1** showing the numbering scheme. The torsion angles [ $^\circ$ ] of the main chain are: N1A-C1A-C2A-N2A 57.9(2), C1A-C2A-N2A-C4A -156.7(2), C2A-N2A-C4A-N1B 177.4(2), N2A-C4A-N1B-C1B 172.6(2), C4A-N1B-C1B-C2B 78.0(3).

urea fragments in the macrocycle present an all-*trans*, planar conformation with all the urea carbonyl groups pointing down and all the NH groups pointing up (Figure 1). The macrocycle exhibits a square shape with a cross-section of 6.052(7) Å (distance between C1A and C1B).

A difference map analysis revealed the presence of two peaks located on the fourfold symmetry axis. The distance between the two peaks was 1.42 Å. NMR experiments gave no evidence for the presence of any organic solvent molecules in the crystal, thus the two peaks were treated as disordered water molecules W1 and W2. The internal van der Waals diameter (approximately 3.5 Å) of the tubular structure is actually large enough to accommodate such molecules. The distance between the two water molecules is too short to have both sites occupied at the same time. There is no short atomic contact favoring hydrogen bonding between the water molecules W1 and W2 and the macrocycle.

The square-shaped cycloureas stack along the crystallographic fourfold axis of the crystal through backbone–backbone hydrogen-bonding interactions so that the two NH hydrogen atoms of each urea fragment interact with a urea oxygen atom of a neighboring macrocycle (Figure 2).

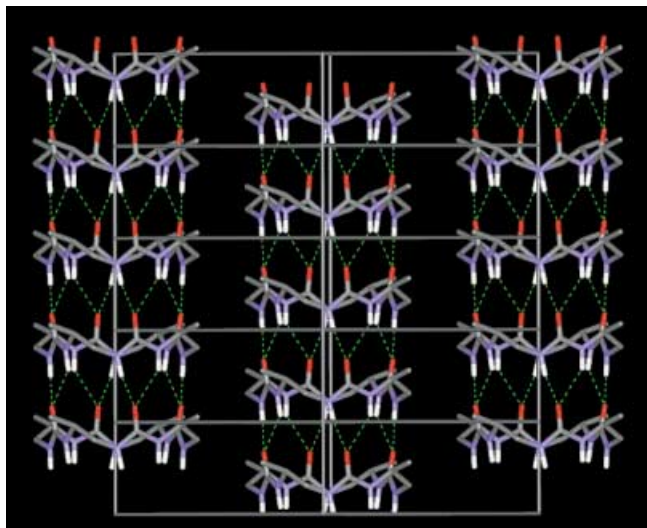


Figure 2. View of the nanotubular organization of **1** along the channel axis. The intermolecular hydrogen bonds are marked as dashed lines. The solvent molecules and H atoms, except those of the NH groups, are omitted for clarity. The edges of the unit cells are represented in gray.

One of the intermolecular N...O distances has standard dimensions (2.798(2) Å), while the other (3.281(2) Å) is just above the limit generally considered for hydrogen-bonding interactions (Figure 2). This stacking of the macrocycles differs from that observed in the crystal structure of cysteine-based macrocyclic bisureas that also exhibits a backbone–backbone urea-type hydrogen-bonding interaction.<sup>[12]</sup> As a consequence of the absence of a local symmetry for the motif C1A–C1B (Figure 1), the urea N–H and C=O bonds in **1** are not parallel to the channel axis and generate two different N...O contacts. Each cyclourea is perpendicular to and centered on the crystallographic quaternary axis in the crystal of **1**. The stacking of the cyclourea units along the crystallographic

*c* axis gives rise to an infinite nanotube. The crystal obtained exhibits a body-centered Bravais lattice, and thus the X-ray structure consists of an array of nanotubes in which each tubular stack is surrounded by four close neighbors at a distance of  $a\sqrt{2}/2$  Å ( $a = 15.333(3)$  Å is one of the unit cell parameters). Neighboring tubes are all arranged in the same direction.<sup>[13]</sup>

The nanotubes are held together in the crystal by loose van der Waals contacts. The intermolecular distances between equivalent C1A atoms and equivalent C3A atoms are 4.097(7) and 4.218(10) Å, respectively.

In summary, we have reported a versatile approach to the synthesis of 20-membered cyclic oligoureas bearing proteinogenic side chains. The cyclic units consisting of homochiral residues self-assemble in the crystal state to form hydrogen-bonded polar nanotubes. The structure of the tubular stack with all the carbonyl and NH groups pointing, respectively, in the same direction is reminiscent of the nanotubes formed by cyclotetra- $\beta$ -peptides with homochiral residues.<sup>[5a]</sup> Particularly noteworthy is the presence of electronic density inside the tubular cavity which was modeled as disordered water molecules at overlapping sites. Further work to explore other tubular arrangements made from cycloureas with different side-chain functionalities and different stereochemistry is on going.

Received: December 18, 2001 [Z18407]

- [1] B. König, *Angew. Chem.* **1997**, *109*, 1919–1921; *Angew. Chem. Int. Ed.* **1997**, *36*, 1808–1832.
- [2] D. T. Bong, T. D. Clark, J. R. Granja, M. R. Ghadiri, *Angew. Chem.* **2001**, *113*, 1016–1041; *Angew. Chem. Int. Ed.* **2001**, *40*, 988–1011, and references therein.
- [3] a) M. R. Ghadiri, J. R. Granja, R. A. Milligan, D. E. McRee, N. Khazanovich, *Nature* **1993**, *366*, 324–327; b) J. R. Granja, R. M. Ghadiri, *J. Am. Chem. Soc.* **1994**, *116*, 10785–10786; c) M. R. Ghadiri, K. Kobayashi, J. R. Granja, R. K. Chadha, *Angew. Chem.* **1995**, *107*, 76–78; *Angew. Chem. Int. Ed.* **1995**, *34*, 93–95.
- [4] Cyclo- $\alpha$ -peptides are stable to proteases and hold great promise as antibacterial agents: S. Fernandez-Lopez, S. H. Kim, E. C. Choi, M. Delgado, J. R. Granja, A. Khasanov, K. Kraehenbuehl, G. Long, D. A. Weinberger, K. M. Wilcoxon, M. R. Ghadiri, *Nature* **2001**, *412*, 392–393.
- [5] a) The structure and tubular stacking of three stereoisomers of cyclo( $\beta^3$ -HAla)<sub>4</sub> have been determined from powder diffraction data: D. Seebach, J. L. Matthews, A. Meden, T. Wessels, C. Baerlocher, L. B. McCusker, *Helv. Chim. Acta* **1997**, *80*, 173–182; b) the structure of the 12-membered-ring cyclo( $\beta^3$ -HGlu)<sub>3</sub> with *S,S,S* configuration investigated by NMR spectroscopy in D<sub>2</sub>O reveals a C<sub>3</sub>-symmetric arrangement with all the carbonyl groups pointing upwards. Modeling experiments suggest that cyclo- $\beta$ -tripeptides can adopt stacked tubular structures: K. Gademann, D. Seebach, *Helv. Chim. Acta* **1999**, *82*, 957–962.
- [6] T. D. Clarck, L. K. Buehler, M. R. Ghadiri, *J. Am. Chem. Soc.* **1998**, *120*, 651–656.
- [7] I. Karle, B. K. Handa, C. H. Hassall, *Acta Crystallogr. B* **1975**, *B31*, 555–560.
- [8] D. Gauthier, P. Baillargeon, M. Drouin, Y. L. Dory, *Angew. Chem.* **2001**, *113*, 4765–4768; *Angew. Chem. Int. Ed.* **2001**, *40*, 4635–4638.
- [9] V. Semetey, D. Rognan, C. Hemmerlin, R. Graff, J.-P. Briand, M. Marraud, G. Guichard, *Angew. Chem.* **2002**, *114*, 1973–1975; *Angew. Chem. Int. Ed.* **2002**, *41*, 1893–1895.
- [10] G. Guichard, V. Semetey, C. Didierjean, A. Aubry, J. P. Briand, M. Rodriguez, *J. Org. Chem.* **1999**, *64*, 8702–8705.

- [11] Crystal data:  $C_{16}H_{32}N_8O_4$ ,  $M_r = 400.48$  g mol<sup>-1</sup>, colorless prism, crystal size  $0.3 \times 0.1 \times 0.1$  mm<sup>3</sup>,  $a = b = 15.333(3)$ ,  $c = 4.724(1)$  Å,  $V = 1110.6(4)$  Å<sup>3</sup>,  $T = 293$  K, tetragonal, space group  $I4$ ,  $Z = 2$ ,  $\rho_{\text{calcd}} = 1.226$  Mg m<sup>-3</sup>,  $\mu = 0.763$  mm<sup>-1</sup>. Nonius Mach3 diffractometer,  $\lambda = 1.54178$  Å. 4293 measured reflections, 1052 unique ( $R_{\text{int}} = 0.017$ ), 953 with  $I > 2\sigma(I)$ , the structure was solved by direct methods and refined by full-matrix least squares on  $F^2$  for all data to  $R_1 = 0.0411$  [ $I > 2\sigma(I)$ ] and  $wR_2 = 0.1036$  [ $I > 2\sigma(I)$ ], 93 parameters. CCDC 175843 contains the supplementary crystallographic data for this paper. These data can be obtained free of charge via [www.ccdc.cam.ac.uk/conts/retrieving.html](http://www.ccdc.cam.ac.uk/conts/retrieving.html) (or from the Cambridge Crystallographic Data Centre, 12, Union Road, Cambridge CB21EZ, UK; fax: (+44) 1223-336-033; or deposit@ccdc.cam.ac.uk).
- [12] Nonsymmetrical macrocyclic bisureas consisting of one cystine unit and one hexamethylenediamine unit bridged together form tubelike hydrogen-bonded aggregates in the solid state. In this case, the carbonyl groups of the two urea units within the same ring point in opposite directions: D. Ranganathan, C. Lakshmi, I. L. Karle, *J. Am. Chem. Soc.* **1999**, *121*, 6103–6107.
- [13] A different packing is observed in the structure of the  $\beta$ -peptide cyclo( $\beta^3$ -HAla)<sub>4</sub> with *S,S,S,S* configuration. Although all C=O and N–H bonds point, respectively, in the same direction in each tubular stack, neighboring tubes are arranged in opposite directions. See reference [5a].

## Drastic Luminescence Response to Carbon Monoxide from a Ru<sup>II</sup> Complex Containing a Hemilabile Phosphane Pyrene Ether\*\*

Carrie W. Rogers and Michael O. Wolf\*

The rapid, reversible nature of the coordinative bonding between metals and Lewis-basic small molecules makes molecular chemosensors based on this phenomenon quite promising. Indeed, recent reviews contain numerous reports of sensors based on metal–ligand interactions.<sup>[1–3]</sup> Of particular potential are metal complexes designed such that the analyte-binding event changes the luminescence properties of an intramolecular lumophore. One approach is to use a modular design in which a metal-based analyte receptor is covalently linked to a separate lumophore. The emission of the lumophore is influenced by the binding of the analyte, usually through On–Off switching of energy- or electron-transfer quenching mechanisms.<sup>[1, 2, 4]</sup> Pyrene, which emits intense indigo-blue fluorescence in dilute solution<sup>[5]</sup> and blue-green excimer emission in concentrated solution,<sup>[5, 6]</sup> is a popular lumophore for such molecule-based sensors, particularly those based on photoinduced electron transfer (PET)

processes.<sup>[2, 7]</sup> Switching between pyrene monomer and excimer emission has also been used to obtain a sensor response, whereby the ability of pyrene moieties to interact with one another is influenced by the binding of analyte to the receptor.<sup>[2, 8]</sup>

We used a [RuCl<sub>2</sub>(POR-*P,O*)<sub>2</sub>] complex (where POR is an ether-substituted phosphane) as the basis for a modular molecular sensor. This type of complex reacts rapidly and reversibly with numerous Lewis-basic small molecules, including CO,<sup>[9–11]</sup> a small-molecule analyte for which effective new sensor materials may be useful, by displacement of the labile ether moiety. Incorporation of a pyrene group in the hemilabile ligand leads to metal-based reactivity towards small molecules and pyrene-based luminescence. Here a Ru<sup>II</sup> complex containing the hemilabile phosphane ether ligand 4-[2-(diphenylphosphanyl)phenoxy]butylpyrene (POC4Pyr) is described. The complex [RuCl<sub>2</sub>(POC4Pyr-*P,O*)<sub>2</sub>] (**1**, see Scheme 1) reacts with carbon monoxide to produce a significant luminescence response in which monomer-to-excimer emission switching is observed. This is the first example of the use of the hemilabile-ligand approach to obtain a molecular sensor with a room-temperature luminescence response, although we have previously reported a Ru bipyridyl complex containing a hemilabile ligand that exhibits small-molecule-dependent luminescence at low temperature.<sup>[12]</sup>

Complex **1** was prepared by reaction of POC4Pyr with RuCl<sub>3</sub>·*x*H<sub>2</sub>O in boiling deaerated ethanol/toluene. The burgundy-pink complex is mildly sensitive to oxidation by air, both in solution and as a solid. The <sup>13</sup>C{<sup>1</sup>H} and <sup>31</sup>P{<sup>1</sup>H} NMR data of **1** (Tables 1 and 2) are analogous to those of [RuCl<sub>2</sub>(POMe-*P,O*)<sub>2</sub>] (POMe = (2-methoxyphenyl)diphenylphosphane), which has been crystallographically characterized<sup>[9]</sup> and found to contain two *P,O*-coordinated phosphane ether ligands with the phosphane moieties *cis* to each other.

The absorption spectrum of complex **1** is essentially a combination of those of [RuCl<sub>2</sub>(POMe-*P,O*)<sub>2</sub>] and the pyrenyl ligand POC4Pyr. The color of the complex is caused by a weak

Table 1. Summary of <sup>13</sup>C{<sup>1</sup>H} NMR spectroscopic data<sup>[a]</sup> for **1–3**.

Complex	CO	$\delta$ /ppm (multiplicity) [J/Hz]		
		<i>ortho</i> <sup>[b]</sup>	<i>ipso</i>	<i>ipso'</i>
<b>1</b>	–	161.7 (t) [5.2]	134.1 (d) [25.3]	ND <sup>[c]</sup>
<b>2</b>	197.6 (t) [13.5]	160.5 (t) [2.3]	132.8 (t) [24.4]	118.8 (t) [23.9]
<b>3</b>	193.7 (t) [10.9]	159.0 (t) [2.3]	131.8 (t) [24]	119.3 (t) [23.5]

[a] In CD<sub>2</sub>Cl<sub>2</sub>. [b] Phenyl C atom bound to oxygen. [c] ND = not determined.

Table 2. Comparison of **1–3** with analogous POMe complexes.<sup>[a]</sup>

Complex	Color	$\delta$ ( <sup>31</sup> P{ <sup>1</sup> H})/ppm	$\tilde{\nu}$ (C=O)/cm <sup>-1</sup>
<i>tcc</i> - <b>1</b>	red	63.7 <sup>[b]</sup>	–
<i>ttt</i> - <b>2</b>	greenish yellow	27.1 <sup>[b]</sup>	2005 <sup>[c]</sup>
<i>cct</i> - <b>3</b>	greenish yellow	13.9 <sup>[b]</sup>	2005, 2058 <sup>[c]</sup>
<i>tcc</i> -[RuCl <sub>2</sub> (POMe- <i>P,O</i> ) <sub>2</sub> ]	red	62.7 <sup>[d]</sup>	–
<i>ttt</i> -[RuCl <sub>2</sub> (CO) <sub>2</sub> (POMe- <i>P</i> ) <sub>2</sub> ]	yellow	26.7	1962
<i>cct</i> -[RuCl <sub>2</sub> (CO) <sub>2</sub> (POMe- <i>P</i> ) <sub>2</sub> ]	white	10.6	2000, 2060

[a] From ref. [9]; <sup>31</sup>P{<sup>1</sup>H} NMR spectra measured in CDCl<sub>3</sub> solution; IR spectra measured in mineral-oil mulls. [b] In CD<sub>2</sub>Cl<sub>2</sub>. [c] In CHCl<sub>3</sub>. [d] In CDCl<sub>3</sub>.

[\*] Prof. M. O. Wolf, C. W. Rogers  
Department of Chemistry, The University of British Columbia  
2036 Main Mall, Vancouver, V6T1Z1 (Canada)  
Fax: (+1) 604-822-2847  
E-mail: mwolf@chem.ubc.ca

[\*\*] This work was supported by the Natural Sciences and Engineering Research Council (NSERC) of Canada. C.W.R. thanks NSERC and UBC for graduate fellowships.

Supporting information for this article is available on the WWW under <http://www.angewandte.com> or from the author.